AMERICAN SOCIETY FOR MICROBIOLOGY | Journal of Virology®

PATHOGENESIS AND IMMUNITY

Covalent Linkage of HIV-1 Trimers to Synthetic Liposomes Elicits Improved B Cell and Antibody Responses

Shridhar Bale,[a] Geraldine Goebrecht,[a] Armando Stano,[a] Richard Wilson,[b] Takayuki Ota,[a] Karen Tran,[b] Jidnyasa Ingale,[a]* Michael B. Zwick,[a] Richard T. Wyatt[a,b,c]

Department of Immunology and Microbiology, Scripps Research Institute, La Jolla, California, USA[a]; International AIDS Vaccine Initiative, Neutralizing Antibody Center, Scripps Research Institute, La Jolla, California, USA[b]; Center for HIV/AIDS Vaccine Immunology and Immunogen Discovery, Scripps Research Institute, La Jolla, California, USA[c]

ABSTRACT We have demonstrated that a liposomal array of well-ordered trimers enhances B cell activation, germinal center formation, and the elicitation of tier-2 autologous neutralizing antibodies. Previously, we coupled well-ordered cleavage-independent NFL trimers via their C-terminal polyhistidine tails to nickel lipids integrated into the lipid bilayer. Despite favorable *in vivo* effects, concern remained over the potentially longer-term *in vivo* instability of noncovalent linkage of the trimers to the liposomes. Accordingly, we tested both cobalt coupling and covalent linkage of the trimers to the liposomes by reengineering the polyhistidine tail to include a free cysteine on each protomer of model BG505 NFL trimers to allow covalent linkage. Both cobalt and cysteine coupling resulted in a high-density array of NFL trimers that was stable in both 20% mouse serum and 100 mM EDTA, whereas the nickel-conjugated trimers were not stable under these conditions. Binding analysis and calcium flux with anti-Env-specific B cells confirmed that the trimers maintained conformational integrity following coupling. Following immunization of mice, serologic analysis demonstrated that the covalently coupled trimers elicited Env-directed antibodies in a manner statistically significantly improved compared to soluble trimers and nickel-conjugated trimers. Importantly, the covalent coupling not only enhanced gp120-directed responses compared to soluble trimers, it also completely eliminated antibodies directed to the C-terminal His tag located at the "bottom" of the spike. In contrast, soluble and noncovalent formats efficiently elicited anti-His tag antibodies. These data indicate that covalent linkage of well-ordered trimers to liposomes in high-density array displays multiple advantages *in vitro* and *in vivo*.

IMPORTANCE Enveloped viruses typically encode a surface-bound glycoprotein that mediates viral entry into host cells and is a primary target for vaccine design. Liposomes with modified lipid head groups have a unique feature of capturing and displaying antigens on their surfaces, mimicking the native pathogens. Our first-generation nickel-based liposomes captured HIV-1 Env glycoprotein trimers via a noncovalent linkage with improved efficacy over soluble glycoprotein in activating germinal center B cells and eliciting tier-2 autologous neutralizing antibodies. In this study, we report the development of second-generation cobalt- and maleimide-based liposomes that have improved *in vitro* stability over nickel-based liposomes. In particular, the maleimide liposomes captured HIV-1 Env trimers via a more stable covalent bond, resulting in enhanced germinal center B cell responses that generated higher antibody titers than the soluble trimers and liposome-bearing trimers via noncovalent linkages. We further demonstrate that covalent coupling prevents release of the trimers prior to recognition by B cells and masks a nonneutralizing determinant located at the bottom of the trimer.

Received 16 March 2017 **Accepted** 30 May 2017

Accepted manuscript posted online 7 June 2017

Citation Bale S, Goebrecht G, Stano A, Wilson R, Ota T, Tran K, Ingale J, Zwick MB, Wyatt RT. 2017. Covalent linkage of HIV-1 trimers to synthetic liposomes elicits improved B cell and antibody responses. J Virol 91:e00443-17. https://doi.org/10.1128/JVI.00443-17.

Editor Guido Silvestri, Emory University

Copyright © 2017 American Society for Microbiology. All Rights Reserved.

Address correspondence to Richard T. Wyatt, wyatt@scripps.edu.

* Present address: Jidnyasa Ingale, ProSci Inc., Poway, California, USA.

KEYWORDS HIV-1, antibody repertoire, human immunodeficiency virus, immunization, immunology, liposomes, nanoparticles, pathogens, vaccines

Vaccine carriers, such as virus-like particles (VLPs), liposomes, nanoparticles, virosomes, and exosomes, in combination with endogenous and/or exogenous adjuvants, display enhanced *in vivo* efficacy of antigen presentation compared to the soluble or monomeric antigen alone. As vaccine candidates, synthetic nanoparticles also provide a safe and efficacious alternative platform to live-attenuated pathogens (1–4). The improved efficacy of synthetic nanoparticles is attributed primarily to their multivalency, stability, and improved circulating half-life *in vivo* (5, 6). Among various vaccine carriers, liposomes have attracted increased interest as a preferred choice for antigen presentation and delivery (7, 8). Numerous strategies have been developed to chemically conjugate antigens to the surfaces of the liposomes, resulting in the stabilization of the antigens and improved presentation of epitopes to immune surveillance (9–11). In addition to vaccine development, the versatile liposomal platform is well suited to a variety of applications, such as targeted drug delivery for cancer therapy, gene delivery, and molecular imaging (12–14).

Recently, we described the development of a first-generation platform for coupling of His-tagged proteins to the surfaces of nickel-bearing liposomes (15). Briefly HIV-1 glycoprotein (Env) trimers are coupled to the liposome by an electrostatic interaction between C-terminal histidine residues of the trimer and Ni^{2+} atoms incorporated into the head group of the phospholipids. Trimers are arrayed at high density on the liposomes, display a native-like antigenic profile, and are stable at 4°C over a period of 6 months. We demonstrated both *in vitro* and *in vivo* that the high density and multivalent array of Env trimers (patient code JRFL, construct SOSIP) on liposomes efficiently activate B cells and generate germinal centers (GC) more efficiently than soluble trimer alone (15). Immunization experiments in rabbits and nonhuman primates revealed a trend in which well-ordered trimers improved tier-2 neutralization, when coupled to liposomes, over the soluble trimers (15, 16).

Antigens coupled to the surfaces of the liposomes are exposed to interstitial and lymphatic fluid as they drain to local lymph nodes and during presentation to B cells (17, 18). In that regard, we note that the antigen coupled to the liposomal surface by noncovalent attachment may dissociate prior to reaching the lymph nodes. To address this concern, we developed a second generation of liposomes that increase the stability of the antigen-liposome coupling.

In this study, we describe the development of liposomes that utilize alternate means to couple HIV-1 Env trimers to synthetic single-bilayer liposomes. We investigated an alternate bivalent metal for chelation to the C-terminal His tags of Env trimers and, as well, optimized maleimide-thiol coupling to covalently attach Env trimers containing C-terminal cysteines to the surfaces of the liposomes. Following conjugation, we characterized the liposomes for trimer antigenicity and stability of the trimer-liposome coupling in EDTA and in mouse serum. We also demonstrated that Env trimer-liposomes (BG505 native flexible linked [NFL] trimers) efficiently activated B cells for enhanced GC formation. Trimers covalently coupled to the liposomes elicited higher antigen-specific IgG titers than soluble trimers or trimers coupled to liposomes via noncovalent metal chelation in two independent experiments. In addition, we also demonstrate that covalent coupling blocks B cell access and antibody elicitation to the "bottom" of the Env spike, indicating that the trimers remain attached to the liposomes during immune recognition and adaptive B cell responses.

RESULTS

Second-generation cobalt- and maleimide-based liposomes. First-generation liposomes employed a noncovalent linkage involving chelation of the His tag by Ni^{2+} and resulted in a high density of Env trimers coating the surfaces of liposomes. The liposomes were comprised of DSPC (1,2-distearoyl-*sn*-glycero-3-phosphocholine), cho-

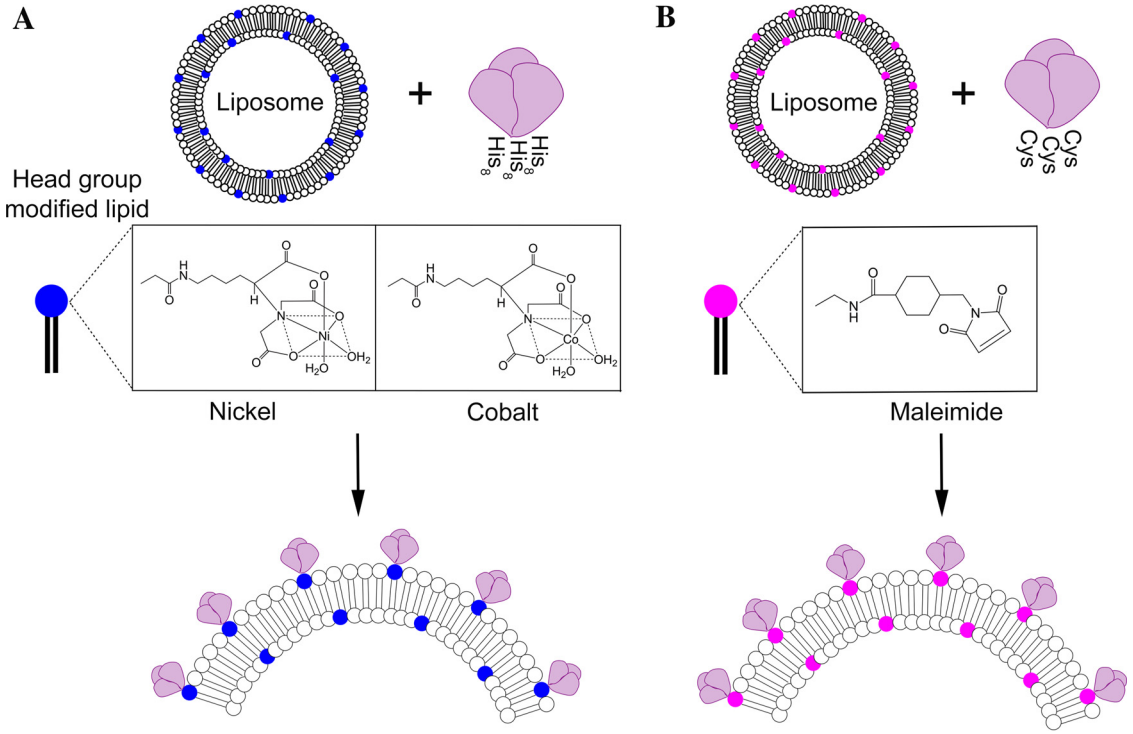

FIG 1 Synthetic nanoparticles as a platform for displaying HIV-1 Env trimers. The schematic shows that liposomes incorporate lipids with modified head groups that mediate coupling of Env trimer to the outer surface. (A) First-generation liposomes contain DGS-NTA in the head group that incorporates nickel or cobalt atoms in the NTA cage, which in turn mediates a noncovalent coupling to a C-terminal His tag of Env trimers. (B) Second-generation liposomes, described here, contain maleimide in the head group that mediates a covalent coupling to a free cysteine group located at the C terminus of each protomeric subunit of each HIV Env trimer.

lesterol, and 1,2-dioleoyl-*sn*-glycero-3-[(*N*-(5-amino-1-carboxypentyl)iminodiacetic acid) succinyl] (nickel salt) [DGS-NTA(Ni^{2+})] at a 60:36:4 molar ratio. Titration of the DGS-NTA(Ni^{2+}) indicated that 4% (molar ratio) was sufficient for optimal occupancy and displayed trimers evenly distributed on the surfaces of the liposomes (15). However, the stability of the trimer-to-liposome linkage has not been thoroughly investigated. Liposomes administered through either the subcutaneous route or the intramuscular route drain through the lymphatic system or circulate through interstitial spaces prior to reaching germinal center B cells. The disassociation of the trimers from the surfaces of the liposomes or degradation of the liposomes *in vivo* before reaching antigen-specific B cells or follicular dendritic cells may limit the benefits of multivalent antigen array and presentation.

To address these potential instability issues, we designed a second generation of liposomes by employing two different strategies: (i) replacing the Ni^{2+} atom in the head group of the liposome with an alternative bivalent chelating atom, cobalt, and (ii) conjugating Env to the liposome via a more stable covalent bond (Fig. 1). DGS-NTA(Co^{2+}) lipid was prepared by conjugating cobalt chloride to DGS-NTA (Avanti Polar Lipids) according to the manufacturer's instructions. Liposomes containing 4% DGS-NTA(Co^{2+}) were prepared using a protocol similar to that described previously for nickel liposomes (15). For a head-to-head comparison, liposomes containing 4% DGS-NTA(Ni^{2+}) were also prepared. BG505 NFL trimers were coupled to both the nickel and cobalt liposomes overnight, purified by size exclusion chromatography (SEC), and visualized by negative-stain electron microscopy (EM) (Fig. 2A). The images indicated that cobalt liposomes load BG505 NFL trimers at a slightly higher density than nickel liposomes.

Maleimide-thiol coupling was employed to introduce a covalent bond between the C-terminal tails of BG505 NFL and the head groups of liposomes. These liposomes (termed "Cys-linked") were composed of DSPC, cholesterol, and 1,2-dipalmitoyl-*sn*-glycero-3-

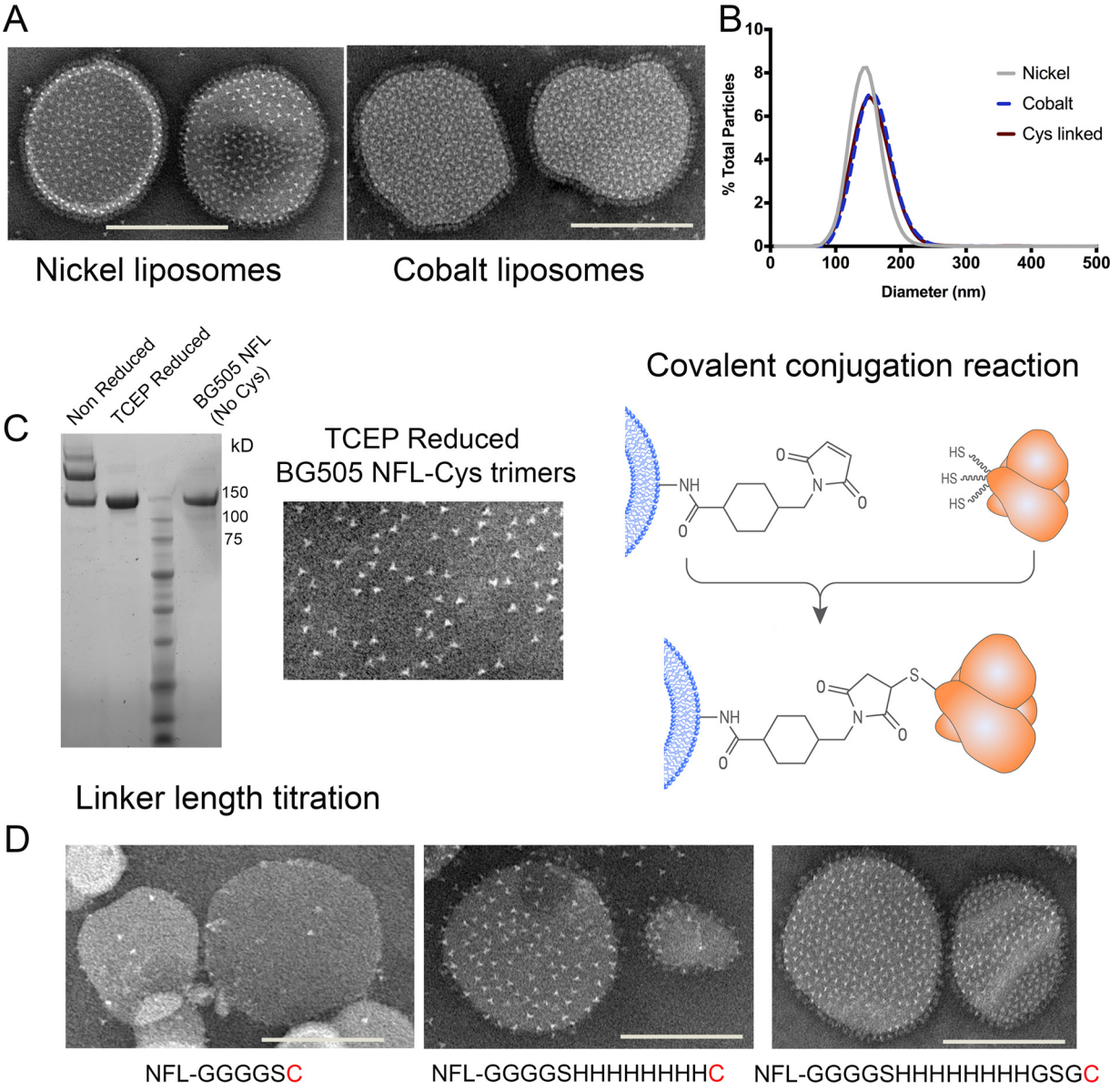

FIG 2 Conjugation of BG505 NFL to second-generation liposomes. (A) Negative-stain EM images of liposomes with nickel in the head group (left) and cobalt in the head group (right) after coupling to BG505 NFL trimers. Bars, ~100 nm. (B) Nanoparticle tracking analysis of liposomes of varying compositions and containing various modified head groups. The diameters of the liposomes ranged from 100 to 220 nm, indicating little variation in particle size distribution. (C) BG505 NFL trimers with a terminal cysteine were reduced with 1 mM TCEP (pH 6.7) prior to coupling. (Left) SDS gel showing that TCEP effectively reduces intertrimer disulfide bonds and results in homogeneous trimers for covalent coupling to liposomes. (Middle) Negative-stain EM image of TCEP-reduced trimers confirming native-like individual trimers. (Right) The covalent-coupling reaction is shown as a schematic. (D) Coupling of BG505 NFL trimers with selected amino acid linker lengths between the C terminus of the gp140 sequence and the terminal cysteine to maleimide liposomes. All the liposomes contained 16% maleimide lipid for conjugating the terminal cysteine residue. The loading of trimers to the liposomes improved with the increasing linker length; left, 5 amino acids [aa]; middle, 13 aa; right, 16 aa. The amino acid sequence of the linker is shown below each image.

phosphoethanolamine-*N*-[4-(*p*-maleimidomethyl)cyclohexane-carboxamide] lipid in a molar ratio of 54:30:16. To investigate the effect of the maleimide lipid on the size distribution of the liposomes postextrusion, we calculated the diameters of all three versions of liposomes using nanoparticle tracking analysis. The mean diameters of various liposomes were in the range of 146 to 159 nm (Fig. 2B), indicating a uniform distribution of liposome size that is not affected by the lipid and cholesterol composition.

A cysteine residue was introduced by site-directed mutagenesis at the C terminus of BG505 NFL, and peptide linkers of various lengths (5, 13, and 16 amino acids) were

introduced between the Env sequence and the terminal cysteine residue. The three forms of BG505 NFL-Cys were expressed and purified in a fashion identical to that for the original non-cysteine-containing trimer. SDS-PAGE analysis revealed that the terminal cysteine residue formed intratrimer disulfide bonds in ~60% of the trimers. Mild reduction by 1 mM tris(2-carboxyethyl)phosphine (TCEP) effectively disrupts intratrimer disulfide bonds, as visualized by SDS-PAGE and EM (Fig. 2C), resulting in homogeneous trimers with free terminal cysteine residues available for coupling to the maleimide liposomes. In addition, the trimers also maintained a closed native-like conformation postreduction, as visualized by EM. The trimers with varying linker lengths were incubated with maleimide liposomes for 72 h, purified by SEC, and visualized by EM. The length of the linker greatly affected loading of BG505 NFL-Cys trimers onto the maleimide liposomes. Optimal loading was empirically determined, guided by the densities achieved by His tag capture. The highest-density array was obtained with the construct that had a 16-amino-acid linker between the end of the Env sequence and the terminal cysteine residue. Moderate loading was observed with the construct that had a 13-amino-acid linker and negligible loading with the 5-amino-acid linker. These results indicated that longer amino acid linkers improve the accessibility of the free cysteine residue for coupling to liposomes (Fig. 2D). Optimal loading was obtained when the liposomes were comprised of 12 to 16% maleimide lipid head groups. The need for an increase in the maleimide lipid compared to the nickel or cobalt lipid to achieve similar trimer densities on the surfaces of the liposomes is unclear. This may be due the efficiency of the cysteine-maleimide covalent linkage versus noncovalent His capture or variation in sorting of the hydrophobic maleimide headgroup between the inner and outer layers of the liposomes or to the fact that TCEP reacts mildly with the maleimde group, rendering some head groups inactive for coupling.

Stability and characterization of the liposomes. We investigated the stability of surface coupling of all three versions of the liposomes with two different approaches, *viz*. (i) the stability of liposomes in mouse serum, mimicking an *in vivo* environment, and (ii) the resistance to stripping of nickel/cobalt by EDTA. To approximate *in vivo* conditions in the lymph, the liposomes were incubated in 20% mouse serum at 37°C and evaluated periodically (0, 1, 4, 24, and 96 h) by negative-stain EM (Fig. 3A). The images revealed sequentially decreasing numbers of trimers on the nickel liposomes over time, indicating that the trimers coupled to nickel liposomes dissociate under these conditions. The nickel liposomes were devoid of detectable surface-conjugated trimers within 96 h after incubation in the 20% mouse serum. However, the trimers on the cobalt- and Cys-linked liposomes remained coupled to the liposomes at densities similar to those of untreated liposomes for up to 96 h in the 20% mouse serum (Fig. 3A).

We next investigated the stability of noncovalent and covalent trimer coupling to the liposomes against stripping of nickel or cobalt atoms from lipid head groups by EDTA compared to the covalently linked trimer-Cys liposomes. We performed this nonphysiologic assay in part to confirm that the covalently linked trimers would remain unaffected by the presence of EDTA. Removal of the nickel/cobalt atoms from the nitrilotriacetic acid (NTA) cage in the head groups of the liposomes by EDTA should result in release of the trimers from the liposome, whereas the covalently linked Cys liposomes should remain unaffected. Nickel/cobalt- and Cys-linked liposomes were incubated in 100 mM EDTA for 30 min, passed over a size exclusion column (to separate liposomes from eluted trimers), and visualized by electron microscopy. BG505 NFL trimers on representative ~100-nm-wide liposomes (measurements were done on two different liposomes postincubation) were counted (Fig. 3B). As expected, incubation with EDTA stripped the nickel-coupled trimers from the liposomes, resulting in a complete loss of trimers from the liposome surface after 30 min. In contrast, and unexpectedly, the cobalt liposomes retained trimers on the liposome surfaces in numbers similar to those retained by Cys-linked liposomes of similar size. Although the reported affinity of NTA is slightly higher for nickel than for cobalt and the affinities for histidine are also similar, the cobalt liposomes appeared resistant to stripping by EDTA.

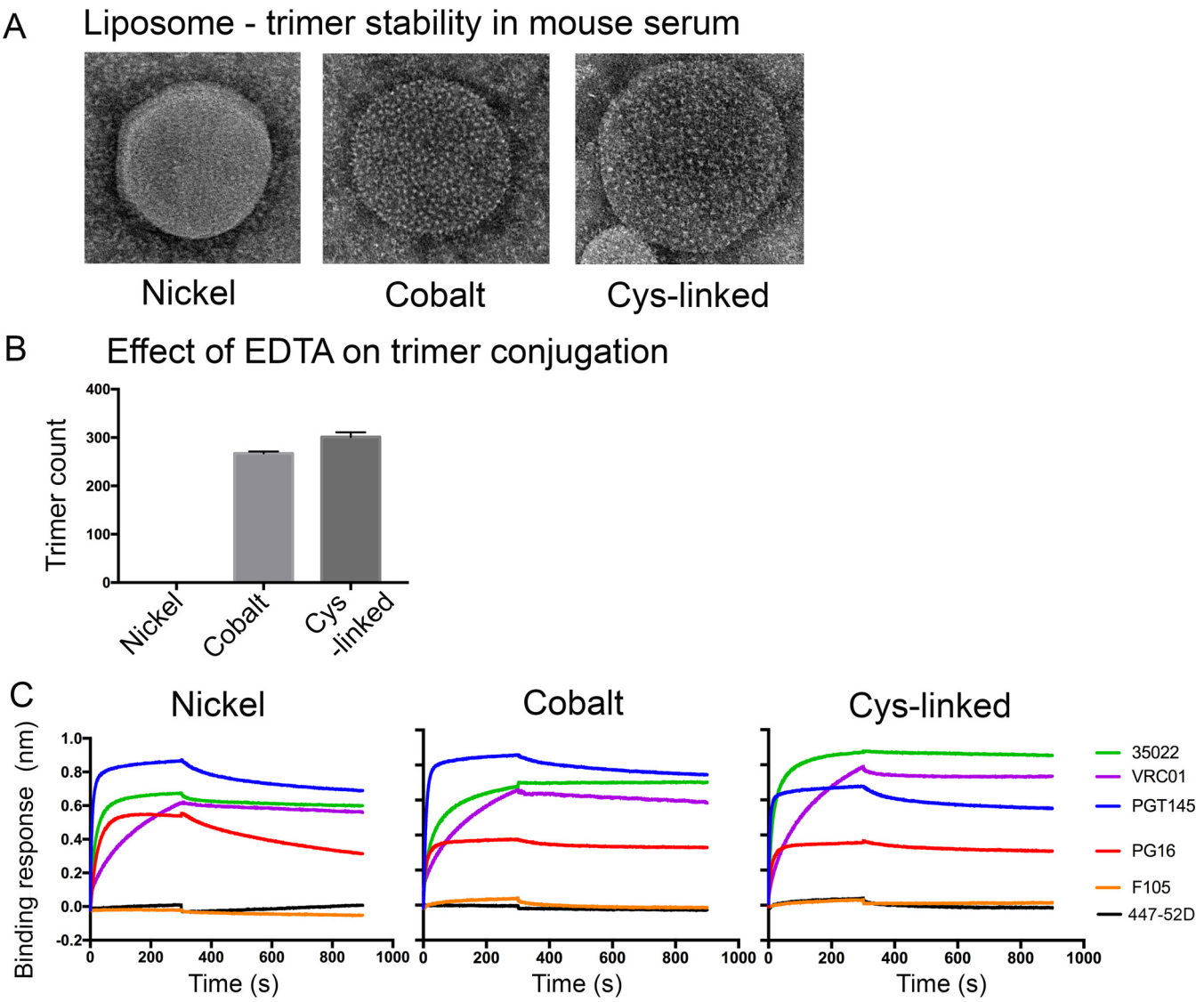

FIG 3 Stability and characterization of BG505 NFL trimers on various liposomes. (A) Liposomes were incubated at 37°C in 20% mouse serum and evaluated for retention of trimers by electron microscopy. Samples were collected after 1 h, 4 h, 24 h, and 96 h (shown). (B) Count of trimers visible by EM on various liposomes after incubation in 100 mM EDTA for 30 min. EDTA strips off surface-coupled trimers on nickel liposomes, but not on cobalt- and Cys-linked liposomes. (C) Biolayer light interferometry (Octet) analysis of binding of trimer-specific bNAbs (PGT145 and PG16), CD4bs bNAbs (VRC01), gp120-gp41 interface bNAb (35022), and non-bNAbs (F105 and 447-52D) to BG505 NFL trimers coupled to nickel-, cobalt-, and Cys-linked liposomes, respectively.

We further investigated the antigenic profile of BG505 NFL trimers captured on the surfaces of the three types of liposomes. For the cysteine-linked trimers, we evaluated recognition of the trimers by selected broadly neutralizing antibodies (bNAbs) and monoclonal antibodies (MAbs) following TCEP reduction by biolayer interferometry analysis (Octet) as previously described (19). In brief, the trimer-liposomes are captured on the surface of the sensor (see Materials and Methods) and probed with selected antibodies to assess relative avidity. The BG505 NFL trimers coupled with nickel, cobalt, or cysteine were efficiently recognized by the trimer-preferring bNAbs PGT145 and PG16 and the CD4 binding site-directed bNAb VRC01 but were not recognized by the nonneutralizing MAb F105 and the V3-specific MAb 447-52D (Fig. 3C). In addition, efficient recognition by the bNAb 35022, which binds to the gp41-gp120 interface, suggested that the epitope of 35022 was accessible to antibody on trimers coupled to the liposomes and might be accessible for B cell recognition (19).

Activation and induction of germinal center B cells by trimer-coupled liposomes. To determine the capacities of the different liposomes to activate B cells, we

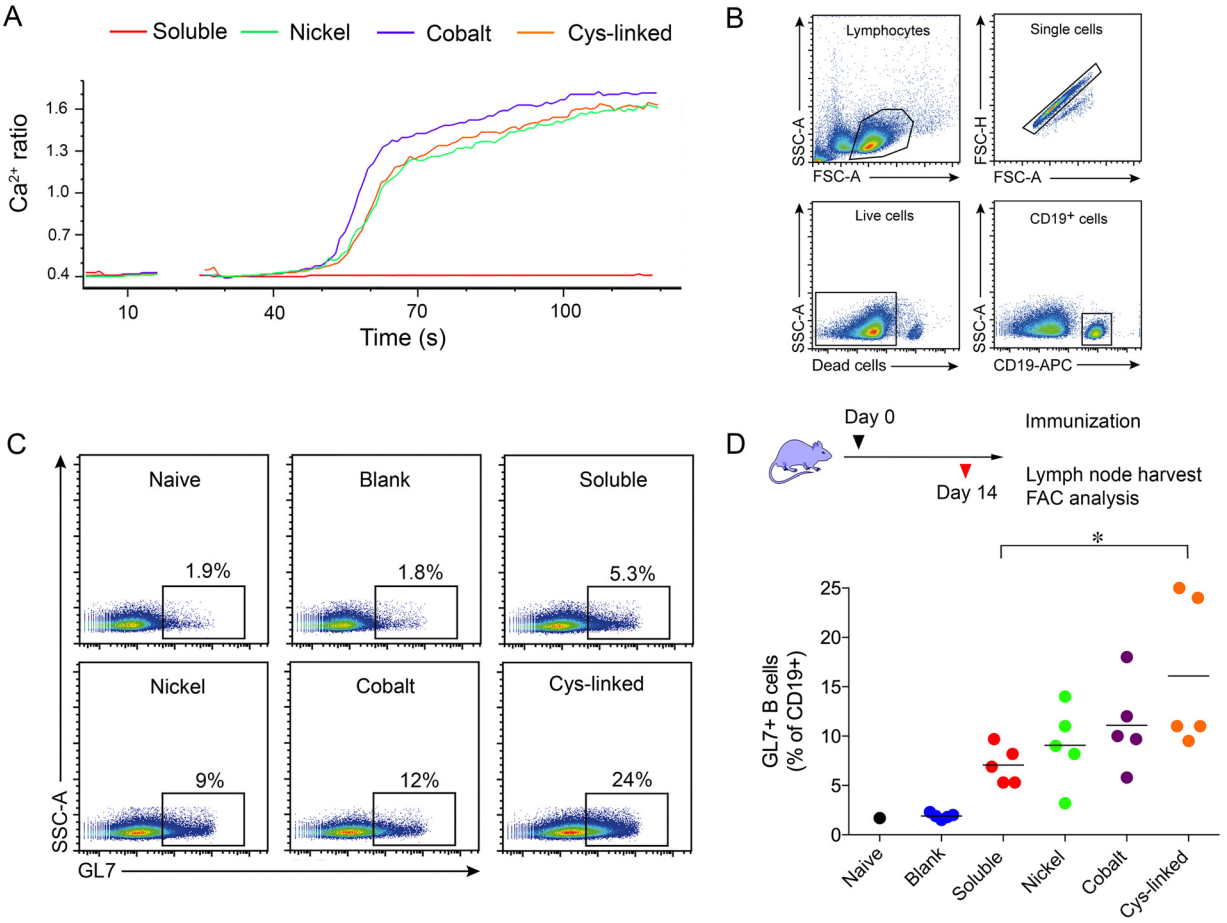

FIG 4 B cells are efficiently activated by BG505 NFL trimers when coupled to liposomes. (A) B cells expressing PGV04 were activated with BG505 NFL trimers either in solution or coupled to various liposomes. The resulting Ca^{2+} flux was measured over a period of 120 s. The trimers activated B cells more effectively when coupled to liposomes (all three versions) than soluble trimers. (B and C) Gating strategy (B) and representative flow cytometry plots (C) analyzing B cells from the draining lymph nodes for the expression of the germinal center marker GL-7. The mice were injected with equal amounts of BG505 NFL trimers, either in solution or coupled to liposomes. The control group received blank liposomes, and a naive mouse was included for comparison. (D) Mice were subcutaneously immunized with soluble trimers and different liposome vaccine formulations. Two weeks postimmunization, B cells from the draining lymph nodes were analyzed for the expression of the germinal center marker GL7. The percentage of $GL7^+$ B cells detected in each gate is shown for each group. A naive mouse and a group of mice administered blank liposomes were used as negative controls. *, $P \leq 0.05$.

measured the *in vitro* calcium flux of a murine B cell line stably expressing the bNAb PGV04, using a flow cytometric assay (20). B cells were simulated with 50 μg/ml of soluble BG505 NFL trimers or liposome-coupled trimers. The resulting Ca^{2+} flux (measurement of a 405/485-nm emission ratio of Indo-1 (2-[4-(bis(carboxymethyl)amino)-3-[2-[2-(bis(carboxymethyl)amino)-5-methylphenoxy]ethoxy]phenyl]-1H-indole-6-carboxylic acid) fluorescence upon excitation by UV) was measured over 120 s. As a result, each of the trimer liposomes generated Ca^{2+} flux responses, while under the conditions used, the soluble trimers generated minimal responses (Fig. 4A). The results indicated that liposome-conjugated BG505 NFL trimers activated the B cells more efficiently than the soluble trimers by cross-linking the B cell receptors (BCRs) (PGV04-BCRs in this case). In addition, the Ca^{2+} flux responses were similar among all the liposome groups, suggesting that the activation gain by avidity is probably dependent on the density of Env trimers on the liposomes and not on the composition of the liposomes or the coupling method.

To determine the *in vivo* capacities of various liposomes to elicit GC B cells, we immunized mice with phosphate-buffered saline (PBS) (naive), plain liposomes (DSPC plus cholesterol), 10 μg of soluble BG505 NFL trimers, or an equivalent amount of BG505 NFL trimers (see Materials and Methods) coupled by nickel, cobalt, or cysteine

linkage. Both soluble and liposome trimers were formulated with 1% Adjuplex (Advanced BioAdjuvants) as an adjuvant. Two weeks after administration, $CD19^+$ B cells from the draining lymph nodes were analyzed for the expression of the GC marker GL7, by flow cytometry (Fig. 4B and C). This analysis showed that the trimer-conjugated liposomes elicited a higher proportion of $GL7^+$ B cells, with the fraction of the $GL7^+$ B cell population increasing as follows: soluble $<$ nickel liposomes $<$ cobalt liposomes $<$ Cys-linked liposomes (Fig. 4D). Mice immunized with Cys-linked liposomes showed the greatest difference from mice immunized with soluble trimers ($P = 0.0346$). These results indicate that covalently linked second-generation liposomal display is at least as effective, if not more effective, at generating $GL7^+$ B cells than the previously described nickel liposomes.

Covalent liposomes elicit increased IgG-binding titers. We next investigated if the improved simulation of B cells in mice resulted in elicitation of increased antigen-specific IgG. Mice (groups of 6 each) were immunized with 10 μg of BG505 NFL trimer in 1% Adjuplex either in soluble format or coupled to liposomes. A control group of three mice received blank liposomes comprised of DSPC and cholesterol only. The mice were immunized at 0, 14, 42, and 70 days, and bleeds were collected 10 days postimmunization (Fig. 5A). To determine overall binding titers in a longitudinal manner, we performed an enzyme-linked immunosorbent assay (ELISA) where the ELISA plate was directly coated with BG505 gp120 or BG505 NFL trimers. This assay showed that Cys-linked liposomes elicited the highest binding IgG titers, as determined by the reciprocal dilution of half-maximal binding (ED_{50}) among all groups following every immunization time (Fig. 5A). All the trimer-liposome-immunized animals from each of these groups generated higher binding IgG titers than the animals from the soluble trimer group, suggesting that the presentation of antigen by particulate array efficiently activates B cells, generating increased GCs and elicitation of serum IgG. In addition, at every time point analyzed, the BG505 NFL trimer bound more IgG in the serum than did BG505 gp120 for animals from all the groups, indicating that mice elicit antibodies against the gp41 region of the trimer. The soluble protein group had negligible IgG-binding titers against gp120 and increased binding titers against the trimer, indicating that mice elicit antibodies preferentially against the gp41 region when vaccinated with the soluble trimer. Similar observations were also made in mice administered BG505 SOSIP, where most of the antibodies were targeted to the base of the trimeric spike (21). After four immunizations (P4), the IgG-binding titers followed the trend Cys-linked $>$ nickel $\approx$ cobalt $>$ soluble against BG505 gp120 and NFL trimer when the ELISA plate was directly coated (Fig. 5B). Importantly, we also demonstrated that none of the mice immunized with either soluble or liposome-coupled BG505 NFL trimers elicited antibodies against the V3 region (as determined by a V3 peptide ELISA [Fig. 5C]). The fact that no V3-directed antibodies were elicited in mice suggests that the V3 region is not exposed *in vivo* in the stable BG505 NFL constructs, consistent with the lack of V3 exposure detected by the antigenic profiling on the liposomes prior to immunization (Fig. 5C). An alternative interpretation is that the mice lack the antibodies in their repertoire specific for the V3 region as presented on the trimer. The latter is unlikely, since Hu et al. detected tier 1 V3-directed neutralizing activity in mice immunized with BG505 SOSIP (21). Perhaps due to the lack of elicitation of V3-directed antibody responses, we did not detect any neutralization activity against the tier 1 isolate SF162 (Tzm-bl assay) (data not shown).

To maintain a more native trimer conformation, we performed binding analysis against BG505 NFL trimers captured by the bNAb 2G12, which is first adsorbed to the ELISA plate. In general, the liposome trimers elicited higher BG505 NFL trimer-specific IgG than did the soluble trimers. In particular, the covalently linked Cys-linked trimers elicited statistically significantly higher binding titers in the mice than did the soluble and nickel liposomes (Fig. 6, P2-P4), consistent with the GC data. In the trimer-Cys-linked immunized animals, all the mice (6/6) responded equally well with little variation in the binding titers between individual mice, whereas greater variation in binding

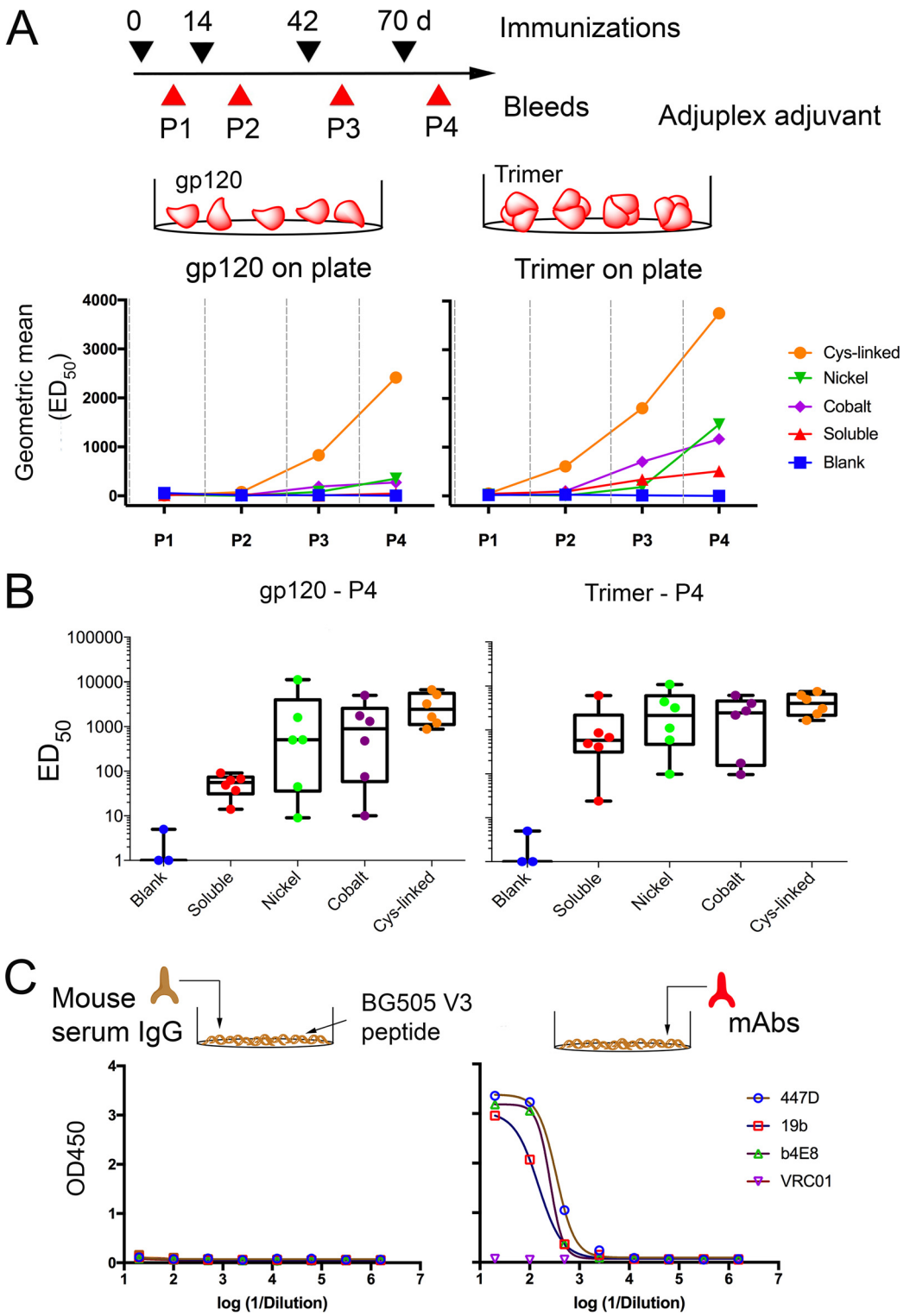

FIG 5 BG505 NFL trimers generate early and improved antigen-specific IgG responses when covalently coupled to liposomes. The schedule of immunizations and bleeds is shown. Each animal received 10 μg of BG505 NFL trimer. (A) Longitudinal analysis of BG505 NFL-specific IgG responses in mice to various groups of liposomes. The geometric mean of the binding titers (ED_{50}) is plotted at every bleed time point. The Cys-linked liposomes generated the highest IgG response to either gp120 (left) or trimer (right) on the ELISA plate at every time point analyzed. The gray dashed lines indicate the immunization time points. (B) ED_{50} binding titers of soluble and various liposome groups after four immunizations (bleed point P4) against BG505 NFL gp120 (left) and BG505 NFL trimer (right). (C) ELISA binding analysis of V3 peptide-specific IgG in mouse serum. ELISA plates were coated with V3 peptide of BG505 Env. Binding was not detected for V3-specific IgG in the sera of all the groups of mice that received BG505 NFL trimers (left) (each symbol represents data for an individual mouse). Control MAbs (at a starting dilution of 10 μg/ml) for V3 peptide binding ELISA are shown on the right.

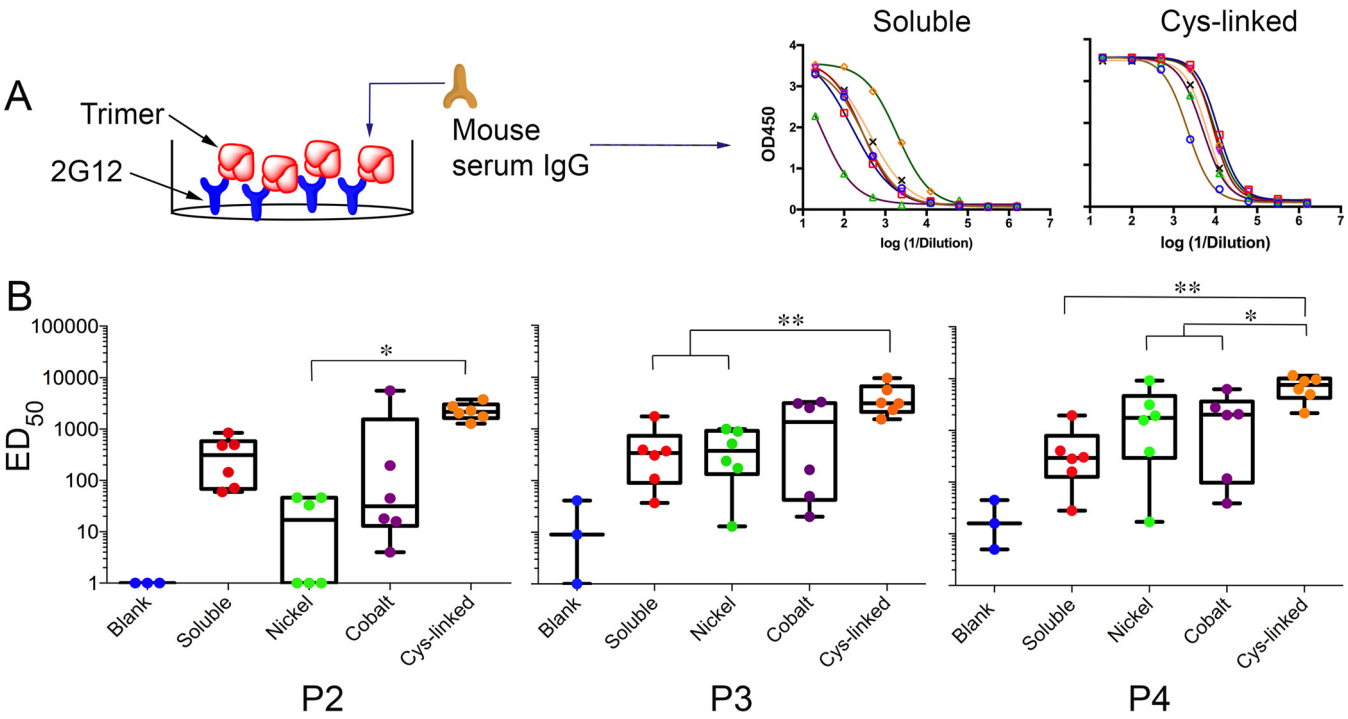

FIG 6 Comparison of BG505 NFL2 trimer-specific responses in all animals on various liposome platforms. Longitudinal analysis is indicated by ED_{50} binding titers of soluble and various liposome groups against BG505 NFL gp140 trimer captured by the glycan-directed bNAb, 2G12, on the wells of the ELISA plate. OD_{450}, optical density at 450 nm. (A) (Left) Cartoon representation of trimer capture via 2G12 on an ELISA plate. (Right) Representative ELISA binding curves. Each symbol/curve represents data from one mouse. (B) The Cys-linked group has the best responses that are uniform across all animals and show a statistically significant difference (ANOVA analysis) from the soluble group or liposome groups with noncovalently coupled trimers. *, $P \leq 0.05$; **, $P \leq 0.01$.

titers was detected for mice immunized with the other immunogens. This was seen for the 2G12-captured trimers and for BG505 gp120 or trimers captured directly on the ELISA plate. While not statistically significant, animals from the trimer-cobalt-liposome group generated higher binding titers than animals from the trimer-nickel-liposome group at all immunization time points.

Effect of adjuvant on the efficacy of liposomes. To investigate the effect of adjuvant on the efficacy of soluble trimer and trimer-liposome presentation, we similarly immunized mice (6 animals/group) with BG505 NFL trimers in solution and coupled to Cys-linked liposomes (the best-responding group in Adjuplex) formulated in Iscomatrix adjuvant. ELISA analysis indicated that the Cys-linked liposomes in Iscomatrix elicited higher BG505 gp120-specific binding titers than did the soluble trimers in a statistically significant manner. Similar trends were seen compared to the Adjuplex adjuvant, but with higher gp120 binding titers elicited by the soluble BG505 NFL trimers formulated in Iscomatrix (Fig. 7). Again, the response was more consistent between individual animals in the trimer-Cys-linked group than with animals from the soluble-trimer group, with a stronger response elicited by covalently linked trimers following 3 inoculations (P3), as well as following 4 inoculations (P4). Despite these efficient binding titers, resulting in saturating ELISA binding curves, we did not detect any BG505 tier autologous neutralization, consistent with a previous report from Hu et al. (21). V3 peptide ELISA with the sera from these mice also revealed undetectable ELISA binding titers (Fig. 5C), indicating that most of the elicited IgG is directed to non-V3 epitopes on the gp120 glycoprotein.

Covalent coupling restricts access to the bottom of the trimer. In principle, coupling to liposomes should restrict accessibility of the polyhistidine tag located in the C-terminal region of BG505 NFL trimers to B cells. However, release of the trimers from the liposome surface (or degradation of the liposomes) would expose the His tag for immune recognition and could result in elicitation of antibodies against this determinant located on the glycan-deficient surface at the "bottom" of the trimer. We used the

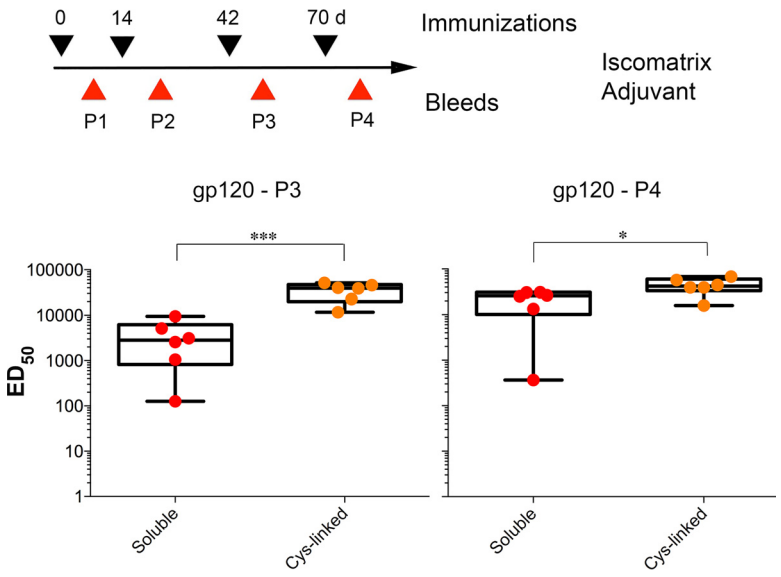

FIG 7 Effect of adjuvant on elicitation of BG505 NFL-specific antibodies. Mice were immunized with soluble BG505 NFL trimers or coupled to Cys-linked liposomes in Iscomatrix adjuvant. ELISA analysis indicated a statistically significant difference in BG505 gp120 binding titers (ED_{50}) between the P3 and P4 time points (Student *t* test). The Cys-linked liposomes generated earlier, better, and more uniform responses to epitopes on gp120 than the soluble trimers. *, $P \leq 0.05$; ***, $P \leq 0.001$.

presence of the His tag on all the immunogens to interrogate antibody responses to this determinant. This analysis should provide additional insights into the relative stability of the trimer-conjugated liposomes. Accordingly, we determined the levels of His tag-specific antibodies present in the sera from all the mice by ELISA. An Ebola virus matrix protein, VP40, possessing a His tag was used as the target for the ELISA analysis. His tag-specific IgG was detected in sera of four out of six mice immunized with soluble BG505 NFL trimers, indicating that mice can elicit antibodies against the polyhistidine tag when it is readily accessible for recognition by B cells. Among the other liposome groups, His tag-specific IgG was detected in sera of four out of six mice from both the trimer-nickel and trimer-cobalt liposome-immunized animals. These data indicated that the His tag becomes accessible to B cells when the trimers are arrayed on the liposomes in a noncovalent manner *in vivo*, likely by dissociation from the liposome. In contrast, there was undetectable His tag-specific IgG binding from any of the six mice immunized with the trimer-Cys-linked liposomes, indicating that covalent linkage restricted access to this immunogenic determinant (Fig. 8). As a negative control, binding of serum IgG to VP40 with a streptavidin tag was not detected in any of the sera (data not shown).

DISCUSSION

Particulate display of antigens (as nanoparticles or VLPs) has several advantages over soluble antigen in activating cellular and humoral responses (22, 23). Here, we developed a liposome platform that covalently captures antigens on the surfaces of the liposomes using a maleimide-thiol bond. We also developed cobalt-based liposomes that capture His-tagged trimers on the surfaces of the liposomes in a noncovalent fashion as an alternative to the previously developed nickel-based liposomes. The newly developed liposomes captured HIV-1 Env BG505 NFL trimers at a high density while maintaining the native-like conformation of the NFL trimers following capture. The newly developed trimer-cobalt and trimer-Cys-linked liposomes were more stable in 20% mouse serum than were the trimer-nickel liposomes. We used 20% serum as a surrogate for lymphatic fluid, which generally has a lower protein content than complete serum. It should be noted, however, that despite the lower stability of the trimer-nickel liposomes as determined by this *in vitro* analysis, we have recently shown

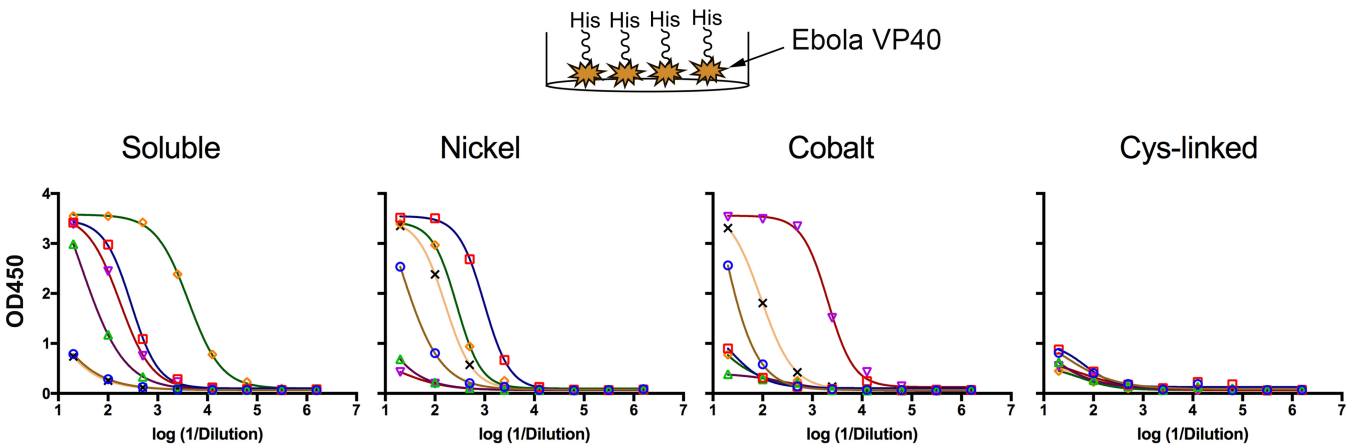

FIG 8 Covalent coupling of BG505 NFL trimer to liposomes restricts accessibility to the bottom of the Env spike. Shown is ELISA binding analysis of His tag-specific IgG in mouse serum (analyzed at P3). The viral matrix protein (VP40) of Ebola virus with a His_6 tag was used as the target for binding IgG. The binding curves indicate low His tag-specific IgG in sera of mice administered Cys-linked liposomes. Each symbol and associated curve represents binding data from one mouse from the corresponding group.

that 16055 NFL-nickel liposomes elicit enhanced autologous tier 2 neutralizing antibodies compared to soluble trimers in nonhuman primates (16). The cobalt- and Cys-linked trimers were also resistant to stripping by EDTA compared to the nickel liposomes. Although this is a nonphysiologic condition, one aim of this analysis was to confirm that covalently linked trimer-Cys liposomes would be unaffected in the presence of EDTA. We did observe this outcome, although somewhat surprisingly, the trimer-cobalt-linked liposomes were also resistant to elution by EDTA.

We show here that liposome-coupled antigens activate B cells more efficiently than the soluble antigen, as determined by Ca^{2+} flux, confirming that avidity from a particulate array can more effectively cross-link BCRs. *In vivo* studies in mice indicated that BG505 NFL trimers resulted in greater expansion of GC B cells when coupled to liposomes than their soluble counterparts. The more stable Cys-linked and cobalt liposomes resulted in a greater GC B cell response than nickel liposomes, suggesting that stability of the antigen coupling to the particles does enhance GC formation in the lymph nodes. The enhanced GC B cell response induced by the Cys-linked liposomes was also associated with more trimer-specific IgG-binding titers in mice (Fig. 6). In addition, the IgG-binding titers in the Cys-linked group of mice are longitudinally statistically significant compared to both the soluble and nickel-based liposomes. Importantly, none of the mice immunized with stable BG505 NFL trimers, either in solution or as an array, elicited antibodies against the immunodominant V3 region in two different adjuvants. Previous studies on BG505 SOSIP have indicated that antibodies elicited against the V3 peptide resulted in tier 1 neutralization, and it was suggested that anti-V3 responses may have distracted the immune system from generation of autologous tier 2 neutralizing antibodies (24). Another study did elicit tier 1 neutralizing antibodies in mice, so the lack of V3-specific antibodies, or detectable tier 1 neutralizing activity, observed here is likely due to the trimer purification procedure used, which negatively selects for any V3-presenting trimers (21).

Our results indicate that the presentation of BG505 NFL as a high-density array on liposomal particles elicits improved B cell responses over soluble versions in mice. Despite these increased binding titers to both BG505 gp120 and the gp140 NFLs, we could not detect BG505 tier 2 autologous neutralizing activity, confirming the results in a previous study from Hu et al. (21). Why mice do not elicit neutralizing antibodies to the glycan hole on BG505 trimers, where these responses are efficiently elicited in rabbits and guinea pigs, is puzzling, but it may be due to repertoire differences, levels of affinity maturation, or other factors regarding how mice process the heavily glycosylated HIV Env trimer.

In sum, we demonstrated that covalent coupling of BG505 NFL to liposomes results

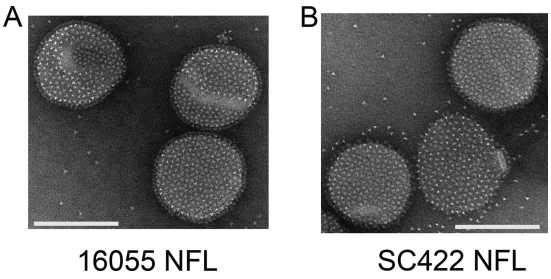

FIG 9 Covalent coupling of other clade Env trimers to Cys-linked liposomes. Shown are negative-stain EM images of 16055 NFL (clade C) (A) and SC422 NFL (clade B) (B) trimers coupled to Cys-linked liposomes. Bars, ~100 nm.

in a stable antigen delivery platform that generates improved and uniform antibody responses in mice. The covalent-coupling method is transferable to NFL Env trimers of other clades that yield stable and native-like trimers (e.g., 16055 NFL and SC422 NFL) (Fig. 9). The stabilized platform of cobalt- and Cys-linked liposomes can potentially improve *in vivo* presentation and efficacy for other protein immunogens that might benefit from particulate display.

MATERIALS AND METHODS

Constructs for protein expression. Our previous work describes in detail the design of the cleavage-independent NFL trimers that yield homogeneous and native-like folded trimers (19). In brief, the NFL design is a single-chain variant of Env where the furin cleavage site is replaced with a flexible linker comprising two copies of G_4S residues and the glycan at the N332 site is restored with a K334S mutation. The C terminus of the protein contains a G_4S linker followed by a His_8 tag to facilitate binding to nickel/cobalt-based liposomes. A BG505 NFL construct containing a cysteine residue at the C terminus was obtained by site-directed mutagenesis (QuikChange Lightning; Agilent Technologies). In addition, linkers comprised of 5, 13, and 16 amino acids were introduced between the terminal cysteine and D664 (the last residue of Env) using the mutagenesis kit.

Purification of BG505 NFL trimers. The purification protocol for BG505 NFL trimers used for this study was previously described (19). Briefly, the plasmid encoding BG505 NFL was transfected into 293F cells (Life Technologies). The supernatants containing protein were harvested 4 days posttransfection and passed over a *Galanthus nivalis* lectin agarose (Vector Laboratories) column for affinity purification. The eluted protein was passed over an S200 size exclusion chromatography column to separate the trimer from aggregated, dimer, and monomeric components. The native and well-folded trimers were further separated from disordered trimers by negative selection using non-bNAb F105, which binds open and disordered trimers (25). The trimer was further purified over an S200 size exclusion column, and the peak fractions containing the trimers were pooled for further analysis.

Generation of trimer-conjugated liposomes. Liposomes for conjugating trimers were prepared as described previously (15). The liposomes were comprised of DSPC (1,2-distearoyl-*sn*-glycero-3-phosphocholine), cholesterol, and a trimer-conjugating lipid, DGS-NTA(Ni^{2+}), DGS-NTA(Co^{2+}), or 1,2-dipalmitoyl-*sn*-glycero-3-phosphoethanolamine-*N*-[4-(*p*-maleimidomethyl)cyclohexane-carboxamide]. The components were mixed in various molar ratios in chloroform and placed overnight in a desiccator under vacuum to yield a lipid film. The film was hydrated in PBS, pH 7.4, for the nickel and cobalt liposomes and in PBS, pH 6.7, for the maleimide liposomes, with vigorous shaking at 37°C followed by sonication for 20 to 30 s. The liposomes were extruded by sequentially passing them 14 to 15 times across a series of membrane filters (Whatman Nuclepore Track-Etch membranes) with pore sizes of 1.0, 0.8, 0.2, and 0.1 μm, respectively. Nanoparticle tracking analysis (NanoSight NS300; Malvern, Ltd., United Kingdom) was used to analyze the size distribution of the liposomes (26). The average diameter of the liposomes was determined by tracking the individual trajectories of a minimum of 2.78×10^5 liposomes per sample, and Nanoparticle tracking analysis 3.1 software was used for the analysis.

The liposomes were incubated overnight with BG505 NFL proteins (900 μg protein for 300 μl liposomes) and passed over a S200 size exclusion column to separate the protein-coupled liposomes from unbound protein. The BG505 NFL protein with a terminal cysteine residue was reduced in 1.0 mM TCEP- PBS, pH 6.7, prior to coupling to maleimide liposomes. The trimer-conjugated liposomes were further purified in a similar way, as mentioned above. The amount of protein conjugated to the liposomes was determined by a Bradford assay using a standard trimer curve generated with the Advanced Protein Assay reagent (Cytoskeleton Inc.) (16).

EM negative staining. Negative-stain EM analysis was done at the core facility at the Scripps Research Institute (TSRI). Liposome samples were applied to glow-discharged carbon-coated mesh (Electron Microscopy Sciences) for 2 min, and the excess sample was removed by blotting to Whatman blotting paper. The grid was transferred onto a droplet of 2% phosphotungstic acid (pH 6.7) for 2 min. The grids were allowed to dry after blotting off the excess stain and examined on a Philips CM100

electron microscope. Liposomes were imaged at various magnifications with a Megaview III charge-coupled-device (CCD) camera.

Characterization and stability of liposomes. The liposomes were incubated in PBS supplemented with EDTA to a final concentration of 100 mM for 30 min at room temperature. The liposomes were separated from free protein by passing over a S200 size exclusion column and visualized by EM. The liposomes were incubated at 37°C in PBS supplemented with 20% mouse serum. Aliquots were removed after 1, 4, 24, and 96 h and viewed under an electron microscope as described above. Control liposomes were incubated in PBS only. Biolayer interferometry (BLI) was used to assess the binding of Abs to trimers conjugated on the liposomes. For BLI, biotinylated wheat germ agglutinin (WGA) (Vector Laboratories) on streptavidin biosensors (ForteBio) was used to capture the trimer-conjugated liposomes according to the manufacturer's instructions and as described previously (15). Binding of MAbs to the immobilized trimers was measured for 300 s, followed by dissociation for 900 s.

Calcium flux assays. The PGV04 WEH-I231 cell line (from David Nemazee's group) was cultured in Advanced Dulbecco's modified Eagle's medium (DMEM) supplemented with 5% fetal calf serum (FCS), 1× penicillin-streptomycin-glutamine, 2 mM GlutaMax-I, and 55 μM 2-mercaptoethanol (2-ME) (20). The cells were treated with 50 ng/μl doxycycline overnight. PGV04 expression was confirmed with human constant chain kappa (hCk) expression by fluorescence-activated cell sorter (FACS). In brief, cells were suspended at 4 million cells/ml in Hanks balanced salt solution (HBSS), labeled with 0.75 μM Indo-1 (Invitrogen) for 30 min at 37°C, and washed with 2 mM $CaCl_2$-HBSS, followed by another 30 min at 37°C. Three hundred microliters of cells at 2 million cells/ml were then stimulated at 37°C with BG505 NFL trimers in solution or coupled to various liposome platforms at a final concentration of 50 μg/ml. Ca^{2+} signals were recorded for 120 s, measuring the 405/485-nm emission ratio of Indo-1 fluorescence upon UV excitation. Calcium flux analysis was performed on an LSR II cytometer (BD Biosciences). Kinetic analysis was performed using FlowJo (Tree Star).

Ethics statement. All experiments were performed at TSRI animal facility, and TSRI Institutional Animal Care and Use Committee (IACUC) approved the study (M1601) and animal-handling protocols. The committee uses the Guide for Care and Use of Laboratory Animals (National Academy Press), Public Health Service (PHS) policy, and the Animal Welfare Act (AWA) as standards. All efforts were made to minimize discomfort to animals during the inoculations and blood collection.

Immunization experiments. C57BL/6 mice (Jackson Laboratory) were inoculated subcutaneously at two sites with 10 μg of soluble trimers or trimers coupled to liposomes formulated in one of the following adjuvants: 1% Adjuplex (Advanced BioAdjuvants) or 1 U Iscomatrix in a total volume of 100 μl. The control group (3 animals) received blank liposomes (DSPC and cholesterol only) formulated similarly to the other groups. Inoculations were done at 0, 2, 6, and 10 weeks. Prebleeds were collected prior to any inoculations, and bleeds were collected 10 days after each inoculation.

Germinal center analysis. The efficiency with which various liposomes activate germinal center B cells was determined using 6-week-old female C57BL/6 mice (5 mice per group). Under isoflurane anesthesia, the mice were administered BG505 NFL trimers (10 μg), either soluble or coupled to liposomes (27), subcutaneously in the hind legs by hock injections. One group of mice received plain liposomes as a negative control. All formulations contained 1% Adjuplex. Two weeks postimmunization, the draining popliteal lymph nodes were harvested and pressed through a 70-μm cell sieve to obtain a single-cell suspension. The cells were labeled with a LIVE/DEAD viability reagent (Invitrogen) to exclude dead cells and with allophycocyanin (APC) anti-mouse CD19 (clone 6D5 for B cells) and fluorescein isothiocyanate (FITC) anti-GL7 (clone GL7 for germinal center B cells) markers (BioLegend). Samples were acquired on a BD LSRII flow cytometer and analyzed using FlowJo software (TreeStar).

ELISA analysis. BG505 NFL-specific, V3 peptide-specific, or His tag-specific IgG-binding titers in mouse serum were determined using ELISA. The 96-half-well ELISA plates (Corning Inc.) were coated overnight at 4°C with BG505 gp120, BG505 NFL, or V3 peptide (at 2 μg/ml) or with bNAb 2G12 (at 1 μg/ml). The plates were blocked for 1 h with blocking buffer comprising 2% nonfat milk in PBS supplemented with 5% fetal bovine serum (FBS). All the plates were washed with PBS supplemented with 0.2% Tween 20 between incubation steps. The plate coated with bNAb 2G12 was incubated with BG505 NFL (at 1.5 μg/ml) in blocking buffer for 1 h to capture the trimers. The plates were incubated for 1 h with 5-fold serial dilutions of serum starting at 1:10 dilution. The plates were further incubated with horseradish peroxidase (HRP)-coupled anti-mouse IgG at 1:5,000 dilution for 1 h and developed with HRP-3,3′,5,5′-tetramethylbenzidine (TMB) substrate solution. The HRP-TMB reaction was stopped with 0.3 N sulfuric acid, and absorbance was measured at 450 nm. To measure the anti-His response in the serum, the plates were initially coated with Ebola virus matrix protein VP40 containing a polyhistidine tag or a streptavidin tag (negative control) and processed as described above. Nonlinear fitting of absorbance data was performed in GraphPad Prism software to obtain half-maximal effective concentration serum binding titers (ED_{50}).

Statistical analysis. Analysis of variance (ANOVA) or Student unpaired *t* test analysis was used for statistical analysis with GraphPad Prism software. Data sets were considered statistically significant at a *P* value of ≤ 0.05.

ACKNOWLEDGMENTS

We thank Malcolm Wood and Theresa Fassel of the Electron Microscopy Core at TSRI for their assistance in sample preparation and image collection and helpful discussions. We thank Viktoriya Dubrovskaya and Shailendra Kumar for the plasmids. We thank Timo Meerloo (UCSD) and Stephen Burgess (Avanti Polar Lipids) for assistance in data

collection and training and for helpful insights. We thank Erica Ollmann Saphire for generously providing Ebola VP40 proteins and Christina Corbaci for assistance in preparation of the figures.

The work is supported by HIVRAD grant P01 AI104722 (S.B., G.G., T.O., and R.T.W.), the Scripps Research Institute grant CHAVI-ID AI100663 (R.T.W.), R01 AI0988602 and the James B. Pendleton Charitable Trust (A.S. and M.B.Z.), and by International AIDS Vaccine Initiative (IAVI) funding (R.T.W., R.W., and K.T.). The full list of donors for IAVI can be found on the website (http://www.iavi.org).

REFERENCES

1. Perrie Y, Mohammed AR, Kirby DJ, McNeil SE, Bramwell VW. 2008. Vaccine adjuvant systems: enhancing the efficacy of sub-unit protein antigens. Int J Pharm 364:272–280. https://doi.org/10.1016/j.ijpharm.2008.04.036.
2. Irvine DJ, Hanson MC, Rakhra K, Tokatlian T. 2015. Synthetic nanoparticles for vaccines and immunotherapy. Chem Rev 115:11109–11146. https://doi.org/10.1021/acs.chemrev.5b00109.
3. Apostolopoulos V. 2016. Vaccine delivery methods into the future. Vaccines (Basel) 4:E9. https://doi.org/10.3390/vaccines4020009.
4. Kushnir N, Streatfield SJ, Yusibov V. 2012. Virus-like particles as a highly efficient vaccine platform: diversity of targets and production systems and advances in clinical development. Vaccine 31:58–83. https://doi.org/10.1016/j.vaccine.2012.10.083.
5. Shen H, Ackerman AL, Cody V, Giodini A, Hinson ER, Cresswell P, Edelson RL, Saltzman WM, Hanlon DJ. 2006. Enhanced and prolonged cross-presentation following endosomal escape of exogenous antigens encapsulated in biodegradable nanoparticles. Immunology 117:78–88. https://doi.org/10.1111/j.1365-2567.2005.02268.x.
6. Mammen M, Choi SK, Whitesides GM. 1998. Polyvalent interactions in biological systems: implications for design and use of multivalent ligands and inhibitors. Angew Chem Int Ed Engl 37:2755–2794.
7. Alving CR, Beck Z, Matyas GR, Rao M. 2016. Liposomal adjuvants for human vaccines. Expert Opin Drug Deliv 13:807–816. https://doi.org/10.1517/17425247.2016.1151871.
8. Liu Y, Chen C. 2016. Role of nanotechnology in HIV/AIDS vaccine development. Adv Drug Deliv Rev 103:76–89. https://doi.org/10.1016/j.addr.2016.02.010.
9. Smith MT, Hawes AK, Bundy BC. 2013. Reengineering viruses and virus-like particles through chemical functionalization strategies. Curr Opin Biotechnol 24:620–626. https://doi.org/10.1016/j.copbio.2013.01.011.
10. Uchida T, Taneichi M. 2014. Application of surface-linked liposomal antigens to the development of vaccines that induce both humoral and cellular immunity. Jpn J Infect Dis 67:235–244. https://doi.org/10.7883/yoken.67.235.
11. Pejawar-Gaddy S, Kovacs JM, Barouch DH, Chen B, Irvine DJ. 2014. Design of lipid nanocapsule delivery vehicles for multivalent display of recombinant Env trimers in HIV vaccination. Bioconjug Chem 25:1470–1478. https://doi.org/10.1021/bc5002246.
12. Vartak A, Sucheck SJ. 2016. Recent advances in subunit vaccine carriers. Vaccines (Basel) 4:E12. https://doi.org/10.3390/vaccines4020012.
13. Yingchoncharoen P, Kalinowski DS, Richardson DR. 2016. Lipid-based drug delivery systems in cancer therapy: what is available and what is yet to come. Pharmacol Rev 68:701–787. https://doi.org/10.1124/pr.115.012070.
14. Grimaldi N, Andrade F, Segovia N, Ferrer-Tasies L, Sala S, Veciana J, Ventosa N. 2016. Lipid-based nanovesicles for nanomedicine. Chem Soc Rev 45:6520–6545. https://doi.org/10.1039/C6CS00409A.
15. Ingale J, Stano A, Guenaga J, Sharma SK, Nemazee D, Zwick MB, Wyatt RT. 2016. High-density array of well-ordered HIV-1 spikes on synthetic liposomal nanoparticles efficiently activate B cells. Cell Rep 15:1986–1999. https://doi.org/10.1016/j.celrep.2016.04.078.
16. Martinez-Murillo P, Tran K, Guenaga J, Lindgren G, Adori M, Feng Y, Phad GE, Bernat NV, Bale S, Ingale J, Dubrovskaya V, O'Dell S, Pramanik L, Spangberg M, Corcoran M, Lore K, Mascola JR, Wyatt RT, Hedestam GBK. 2017. Particulate array of well-ordered HIV clade C Env trimers elicits neutralizing antibodies that display a unique V2 cap approach. Immunity 46:804–817. https://doi.org/10.1016/j.immuni.2017.04.021.
17. Allen TM, Hansen CB, Guo LS. 1993. Subcutaneous administration of liposomes: a comparison with the intravenous and intraperitoneal routes of injection. Biochim Biophys Acta 1150:9–16. https://doi.org/10.1016/0005-2736(93)90115-G.
18. Velinova M, Read N, Kirby C, Gregoriadis G. 1996. Morphological observations on the fate of liposomes in the regional lymph nodes after footpad injection into rats. Biochim Biophys Acta 1299:207–215. https://doi.org/10.1016/0005-2760(95)00208-1.
19. Sharma SK, de Val N, Bale S, Guenaga J, Tran K, Feng Y, Dubrovskaya V, Ward AB, Wyatt RT. 2015. Cleavage-independent HIV-1 Env trimers engineered as soluble native spike mimetics for vaccine design. Cell Rep 11:539–550. https://doi.org/10.1016/j.celrep.2015.03.047.
20. Ota T, Doyle-Cooper C, Cooper AB, Huber M, Falkowska E, Doores KJ, Hangartner L, Le K, Sok D, Jardine J, Lifson J, Wu X, Mascola JR, Poignard P, Binley JM, Chakrabarti BK, Schief WR, Wyatt RT, Burton DR, Nemazee D. 2012. Anti-HIV B cell lines as candidate vaccine biosensors. J Immunol 189:4816–4824. https://doi.org/10.4049/jimmunol.1202165.
21. Hu JK, Crampton JC, Cupo A, Ketas T, van Gils MJ, Sliepen K, de Taeye SW, Sok D, Ozorowski G, Deresa I, Stanfield R, Ward AB, Burton DR, Klasse PJ, Sanders RW, Moore JP, Crotty S. 2015. Murine antibody responses to cleaved soluble HIV-1 envelope trimers are highly restricted in specificity. J Virol 89:10383–10398. https://doi.org/10.1128/JVI.01653-15.
22. Schiller J, Chackerian B. 2014. Why HIV virions have low numbers of envelope spikes: implications for vaccine development. PLoS Pathog 10:e1004254. https://doi.org/10.1371/journal.ppat.1004254.
23. Zhao C, Ao Z, Yao X. 2016. Current advances in virus-like particles as a vaccination approach against HIV infection. Vaccines (Basel) 4:E2. https://doi.org/10.3390/vaccines4010002.
24. Sanders RW, van Gils MJ, Derking R, Sok D, Ketas TJ, Burger JA, Ozorowski G, Cupo A, Simonich C, Goo L, Arendt H, Kim HJ, Lee JH, Pugach P, Williams M, Debnath G, Moldt B, van Breemen MJ, Isik G, Medina-Ramirez M, Back JW, Koff WC, Julien JP, Rakasz EG, Seaman MS, Guttman M, Lee KK, Klasse PJ, LaBranche C, Schief WR, Wilson IA, Overbaugh J, Burton DR, Ward AB, Montefiori DC, Dean H, Moore JP. 2015. HIV-1 vaccines. HIV-1 neutralizing antibodies induced by native-like envelope trimers. Science 349:aac4223. https://doi.org/10.1126/science.aac4223.
25. Guenaga J, de Val N, Tran K, Feng Y, Satchwell K, Ward AB, Wyatt RT. 2015. Well-ordered trimeric HIV-1 subtype B and C soluble spike mimetics generated by negative selection display native-like properties. PLoS Pathog 11:e1004570. https://doi.org/10.1371/journal.ppat.1004570.
26. Wright M. 2012. Nanoparticle tracking analysis for the multiparameter characterization and counting of nanoparticle suspensions. Methods Mol Biol 906:511–524. https://doi.org/10.1007/978-1-61779-953-2_41.
27. Kamala T. 2007. Hock immunization: a humane alternative to mouse footpad injections. J Immunol Methods 328:204–214. https://doi.org/10.1016/j.jim.2007.08.004.